



Title:

Topology Optimization for Design of Hybrid Lattice Structures with Multiple Functional Microstructure Configurations

Authors:

Yifan Guo, guo15@ualberta.ca, University of Alberta

Yongsheng Ma, mays@sustech.edu.cn, Southern University of Science and Technology

Rafiq Ahmad, Rafiq.Ahmad@ualberta.ca, University of Alberta

Keywords:

Topology optimization, Hybrid lattice structures, thermal expansion

DOI: 10.14733/cadconfP.2022.271-276

Introduction:

Lattice structures (LSs) have been an emerging solution toward lightweight and mechanically efficient structures [2-3]. However, while the lattice structure presents a vast design space and advantage, it also poses a challenge to existing design methods. Existing LSs design methods rarely consider microstructures with functionalities, like negative Poisson's ratio [8] and extreme thermal expansion [5]; Therefore, this work proposes a method based on topology optimization and homogenization theory to design hybrid lattice structures with multiple functional microstructure configurations to fill the gap in the design approach for multi-functional lattice structures. The flow chart of the proposed method is shown in Fig 1. There are two steps in this method. At first, multiple functional microstructure lattice units are obtained through topology optimization and homogenization theory. Then, the microstructures are treated as homogeneous materials with effectively homogenized properties for macroscopic analysis, and the ordered SIMP (Solid isotropic material with penalization) interpolation method [7] is applied to achieve the interpolation of multiple microstructures. Finally, the obtained hybrid lattice structure theoretically has both the properties of macroscopic optimization and the functionalities of microstructure units. Both the microstructure and macrostructure design variables are updated by the Method of Moving Asymptote (MMA) algorithm [4].

To verify this proposed method, an optimization model that the functional microstructure is set to be zero thermal expansion coefficient, and a standard minimized compliance problem is considered in macroscale is created. Numerical examples and data comparisons are presented.

Main Idea:

Functional microstructure design with Zero thermal expansion

In this section, a numerical procedure for 2D thermal elastic microstructure topology optimization of three-phase materials (two solid and one void materials, the properties are shown in Tab.1.) is introduced, whose optimization model can be expressed as:

$$\left\{ \begin{array}{l} \min: f(x,y) = (\alpha_{11}^H(x,y))^2 + (\alpha_{22}^H(x,y))^2 \\ \text{subject to: } \left\{ \begin{array}{l} V_x = \frac{1}{V} \sum_{e=1}^{NE} x_e (1-y_e) V_e; V_1^{Low} \leq V_x \leq V_1^{Up} \\ V_y = \frac{1}{V} \sum_{e=1}^{NE} x_e y_e V_e; V_2^{Low} \leq V_y \leq V_2^{Up} \\ K \geq K_{set} \end{array} \right. \end{array} \right. \quad (1)$$

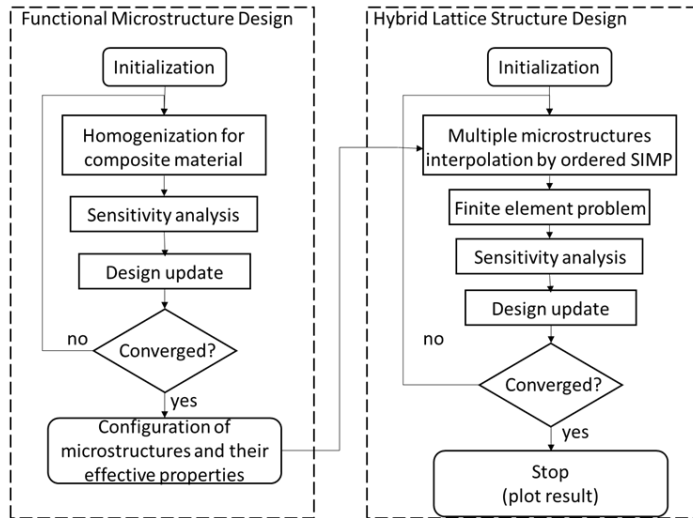


Fig. 1: Flow chart of the proposed method.

	Young's moduli E^i	Passion ratio ν	Thermal expansion coefficient α^i
solid material 1	145MPa	0.3	0.5×10^{-4}
solid material 2	290MPa	0.3	2.2×10^{-4}

Tab. 1: The mechanical properties of solid material.

where α_{ii}^H ($i = 1$ or 2) is the effective thermal expansion tensor. V_x and V_y are two volume fractions for two solid materials. V is the volume of the whole domain. V_e is the volume of the element. NE is the number of elements. x_e and y_e are two local design variables for two solid materials. To avoid singularity, the "void" phase is taken as a small number 10^{-4} times material tensors of phase solid material 1. V_i^{Low} and V_i^{Up} ($i = 1$ or 2) is the predefined upper and lower volume fraction limits. Generally, zero thermal expansion design is usually achieved at the expense of the overall stiffness of the composite. Thus, a lower bound constraint on the overall composite stiffness ($K \geq K_{set}$) is introduced here to ensure the composite stiffness performance. K indicates the effective bulk moduli, which can be expressed in terms of the components of the effective elasticity tensor C^H .

$$K = 0.25C_{11}^H + 0.25C_{12}^H + 0.25C_{21}^H + 0.25C_{22}^H \quad (2)$$

and K_{set} is the prescribed minimum bulk moduli value.

The effective properties of the microstructure can be obtained by using homogenization theory [1]; the effective elasticity tensor C_{pqrs}^H and thermal strain tensor β_{pq}^H can be written as:

$$\mathbf{C}_{pqrs}^H = \frac{1}{|Y|} \int_Y \mathbf{C}_{pqrs}^e (\varepsilon_{pq}^0 - \varepsilon_{pq}) (\varepsilon_{rs}^{0(ji)} - \varepsilon_{rs}^{ij}) dy \quad (3)$$

$$\beta_{pq}^H = \frac{1}{|Y|} \int_Y \mathbf{C}_{pqrs}^e (\alpha_{pq} - \varepsilon_{pq}^\alpha) (\varepsilon_{rs}^{0(ji)} - \varepsilon_{rs}^{ij}) dy \quad p, q, r, s = 1, 2. \quad (4)$$

where $|Y|$ denotes the volume of the unit cell and ε^0 is known as a test strain field. ε is the virtually local strain field. \mathbf{C}_{ijpq}^e and α_{pq} are the locally varying stiffness tensor and local thermal strain tensor, respectively, which can be interpolated by the extended SIMP interpolation scheme; it can be formulated as:



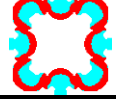
$$\mathbf{C}_{ijpq}^e(x_e, y_e) = x_e^{P1} \cdot (y_e^{P1} \cdot \mathbf{C}_{ijpq}^2 + (1 - y_e)^{P1} \cdot \mathbf{C}_{ijpq}^1) \quad (5)$$

$$\alpha_{ij} = y_e^{P1} \cdot \alpha_{ij}^2 + (1 - y_e)^{P1} \cdot \alpha_{ij}^1 \quad (6)$$

where \mathbf{C}_{ijpq}^j and α_{ij}^j ($j = 1$ or 2) are represented stiffness tensor and thermal strain coefficient tensor for solid material 1 and solid material 2, respectively. P1 is the penalty coefficient. The equivalent thermal expansion tensor α_{ij}^H can be calculated by:

$$\alpha_{ij}^H = (\mathbf{C}_{pqrs}^H)^{-1} \beta_{pq}^H \quad (7)$$

Finally, three designed zero thermal expansion microstructures with different volume fractions are shown in below table:

	V_x	V_y	Configuration	Bulk moduli K	Objective function f	Effective elastic tensor \mathbf{C}_{pqrs}^H
Microstructure1	0.2	0.2		100	$0.8787E-5$	$\begin{bmatrix} 112.55 & 87.44 & 0 \\ 87.44 & 112.55 & 0 \\ 0 & 0 & 48.88 \end{bmatrix}$
Microstructure2	0.25	0.25		150	$0.1395E-5$	$\begin{bmatrix} 186.44 & 113.56 & 0 \\ 113.56 & 186.44 & 0 \\ 0 & 0 & 85.25 \end{bmatrix}$
Microstructure3	0.3	0.3		200	$0.2747E-5$	$\begin{bmatrix} 261.85 & 138.44 & 0 \\ 138.44 & 261.85 & 0 \\ 0 & 0 & 48.88 \end{bmatrix}$

Tab. 2: The mechanical properties of three pre-designed microstructures.

Hybrid lattice structure design based on ordered SIMP

This section describes the topology optimization in macroscale; the optimization model can be expressed as:

$$\begin{cases} \min: c(\rho) = \mathbf{u}^T \mathbf{K} \mathbf{u} = \sum_{e=1}^{NE} \mathbf{u}_e^T \mathbf{k}_e(\rho_e) \mathbf{u}_e \\ \text{subject to: } \begin{cases} \mathbf{K} \mathbf{U} = \mathbf{F} \\ V(\rho)/V_0 \leq VF_{set} \\ 0 \leq \rho \leq 1 \end{cases} \end{cases} \quad (8)$$

where c is the macroscale structural compliance; ρ is the vector of element densities, \mathbf{K} , \mathbf{U} , and \mathbf{F} are the global stiffness matrix, displacement vector, and force vector, respectively; $V(\rho)$ and V_0 are the material volume and design domain volume, and VF_{set} is the prescribe volume fraction. \mathbf{k}_e is the elementary stiffness matrix, which can be expressed by:

$$\mathbf{k}_e = \mathbf{B}^T \mathbf{C}_e \mathbf{B} \quad (9)$$

\mathbf{B} denotes the strain-displacement matrix, and \mathbf{C}_e is the homogenized elastic tensor obtained from the previous section. In this work, the designed functional microstructures are anisotropic; all the elastic tensor terms could be interpolated by ordered SIMP.

In ordered SIMP, multi-microstructures are sorted in the ascending order of their corresponding material density ρ_i^T . Then, the material densities are normalized as:

$$\rho_i = \frac{\rho_i^T}{\rho_{\max}} \quad (10)$$

ρ_{\max} is the density for the stiffest microstructure; it should be noted that the density of two solid materials that compose the microstructure is assumed to be the same, so the density of the corresponding microstructure is determined by the sum volume fraction of two solid materials. The three microstructures with three normalized densities $\rho_i = [0, \frac{2}{3}, \frac{5}{6}, 1]$ shown in Tab.2. are all used in this work, then the elastic tensor is presented below,

$$\mathbf{C}_e = \eta(\rho_e) \cdot \mathbf{C}_{\max}^H = \begin{bmatrix} \eta_{11}^E(\rho_e) \cdot C_{11}^H & \eta_{12}^E(\rho_e) \cdot C_{12}^H & 0 \\ \eta_{21}^E(\rho_e) \cdot C_{21}^H & \eta_{22}^E(\rho_e) \cdot C_{22}^H & 0 \\ 0 & 0 & \eta_{33}^E(\rho) \cdot C_{33}^H \end{bmatrix} \quad (11)$$

where \mathbf{C}_{\max}^H is the elastic tensor for the stiffest microstructure, $\eta(\rho_e)$ is the ordered SIMP interpolation function, which is given as:

$$\eta(\rho_e) = \left(\frac{\rho_e - \rho_i}{\rho_{i+1} - \rho_i} \right)^{P2} \cdot \left(\frac{C_{i+1}^H - C_i^H}{C_{\max}^H} \right) + \frac{C_i^H}{C_{\max}^H}, \rho_e \in [\rho_i, \rho_{i+1}] \quad (12)$$

where C_i^H indicates the elastic tensor of the i^{th} microstructure; $P2$ is the penalty coefficient in ordered SIMP interpolation.

Case study:

In this section, the proposed method is validated with a classical 2-D L-bracket benchmark, as shown in 0. In this example, 4-node quadrilateral elements are adopted. The top edge of the L-bracket is clamped, and a vertical load $F=4500\text{N}$ is exerted to the right-side upper corner. Note that the load is distributed over six nodes to avoid stress concentration. The initial value of design variables is set to be 0.3, and the filter radius is 3.5 element sizes. The iterative process will terminate when no further improvement of the objective function can be achieved. Namely, the difference of the objective values between two adjacent iterations is less than 0.01 in 20 steps, or the maximum iteration number (450) is exceeded.

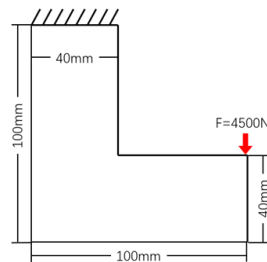


Fig. 2: The boundary conditions for the L-Bracket.

Fig. 3 (a). presents the microstructure distribution and optimal structure. The structure thermal distortion under temperature change $30\text{ }^{\circ}\text{C}$ is shown in **Error! Reference source not found.** (b). The maximum displacement is 0.0255 mm , and the compliance of the whole structure is $c = 2.5725$. To make

a comparison, Fig. 3(c). shows the optimal result only with solid material 1 under the same volume fraction ($VF_{Set} = 0.5$), and the compliance is $c = 3.1572$. The maximum thermal distortion is 0.2427 mm , as indicated in Fig. 3 (d). The experiment results validate that the proposed method could design structures with higher stiffness and substantially reduced structural thermal distortion compared to the structure optimized with the conventional approach. Fig.4. presents the Full-scale structure of optimal result with multi-microstructures.

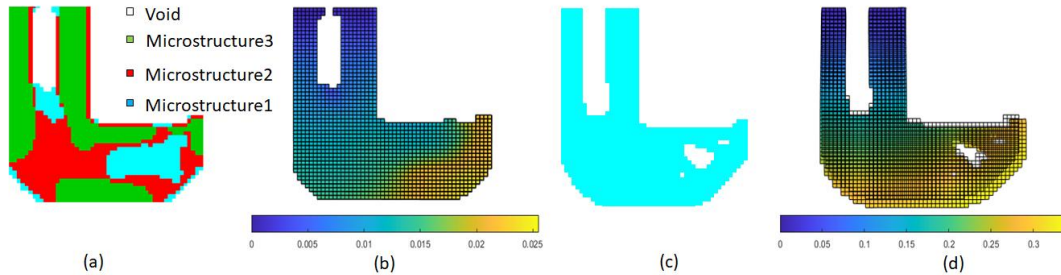


Fig. 3: (a)The optimal result with multi-microstructures and (b) its thermal expansion ($\Delta T=30^{\circ}\text{C}$); (c) The optimal result only with solid material 1 and (b) its thermal expansion ($\Delta T=30^{\circ}\text{C}$).

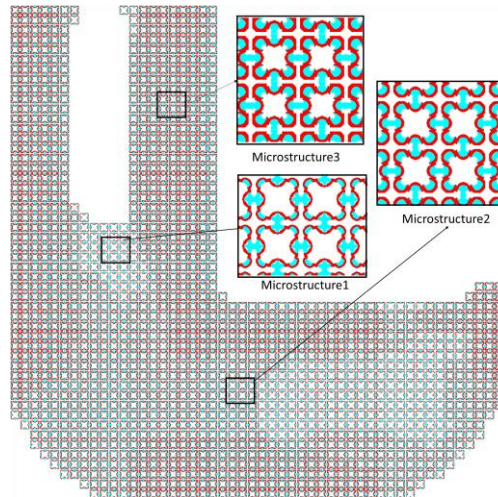


Fig. 4: Full-scale structure.

Conclusion:

This work proposed a method based on topological optimization and homogenization theory to design hybrid lattice structures with multiple functional microstructure configurations. To verify the effectiveness of this approach, microstructures with zero thermal expansion were obtained in this work, and it is used to design the optimal stiffness hybrid lattice structure. The final case study shows the structure obtained by this method did have the advantage of being more stiffness and less thermally expanded than the results obtained from the optimization of pure materials.

References:

- [1] Andreassen, E.; Andreassen, C. S.: How to determine composite material properties using numerical homogenization, Computational Materials Science, 83, 2014, 488-495 , <https://doi.org/10.1016/j.commatsci.2013.09.006>

- [2] Cheng, L.; Liu, J.; Liang, X.; To, A. C.: Coupling lattice structure topology optimization with design-dependent feature evolution for additive manufactured heat conduction design, *Computer Methods in Applied Mechanics and Engineering*, 332, 2018, 408-439, <https://doi.org/10.1016/j.cma.2017.12.024>
- [3] Cheng, L.; Zhang, P.; Biyikli, E.; Bai, J.; Robbins, J.; To, A.: Efficient design optimization of variable-density cellular structures for additive manufacturing: theory and experimental validation, *Rapid Prototyping Journal*, 2017, <https://doi.org/10.1108/RPJ-04-2016-0069>
- [4] Svanberg, K.: The method of moving asymptotes—a new method for structural optimization, *International Journal for Numerical Methods in Engineering*, 24, 1987, 359-373 , <https://doi.org/10.1002/nme.1620240207>
- [5] Sigmund, O.; Torquato, S.: Design of materials with extreme thermal expansion using a three-phase topology optimization method, *Journal of the Mechanics and Physics of Solids*, 45, 1997, 1037-1067, [https://doi.org/10.1016/S0022-5096\(96\)00114-7](https://doi.org/10.1016/S0022-5096(96)00114-7)
- [6] Wei, N.; Ye, H.; Zhang, X.; Li, J.; Sui, Y.: Topology Optimization for Design of Hybrid Lattice Structures with Multiple Microstructure Configurations, *Acta Mechanica Solida Sinica*, 2022, 1-17 , <https://doi.org/10.1007/s10338-021-00302-3>
- [7] Xu, S.; Liu, J.; Zou, B.; Li, Q.; Ma, Y.: Stress constrained multi-material topology optimization with the ordered SIMP method, *Computer Methods in Applied Mechanics and Engineering*, 373, 2021, 113453, <https://doi.org/10.1016/j.cma.2020.113453>
- [8] Xie, Y. M.; Yang, X.; Shen, J.; Yan, X.; Ghaedizadeh, A.; Rong, J.; Huang, X.; Zhou, S.: Designing orthotropic materials for negative or zero compressibility, *International Journal of Solids and Structures*, 51, 2014, 4038-4051, <https://doi.org/10.1016/j.ijsolstr.2014.07.024>